Influence of indium clustering on the band structure of semiconducting ternary and quaternary nitride alloys

I. Gorczyca, S. P. Łepkowski, and T. Suski
Institute of High Pressure Physics, Polish Academy of Sciences, Sokolowska 29/37, 01-142 Warsaw, Poland

N. E. Christensen and A. Svane
Department of Physics and Astronomy, Aarhus University, DK-8000 Aarhus C, Denmark
(Received 10 April 2009; revised manuscript received 23 June 2009; published 5 August 2009)

The electronic band structures of $In_xGa_{1-x}N$, $In_xAl_{1-x}N$, and $In_xGa_yAl_{1-x-y}N$ alloys are calculated by *ab initio* methods using a supercell geometry, and the effects of varying the composition and atomic arrangements are examined. Particular attention is paid to the magnitude of and trends in bowing of the band gaps. Indium composition fluctuation (clustering) is simulated by different distributions of In atoms and it is shown that it strongly influences the band gaps. The gaps are considerably smaller when the In atoms are clustered than when they are uniformly distributed. An explanation of this phenomenon is proposed on the basis of an analysis of the density of states and the bond lengths, performed in detail for ternary alloys. Results for the band gaps of $In_xGa_yAl_{1-x-y}N$ quaternary alloys show a similar trend. It is suggested that the large variation in the band gaps determined on samples grown in different laboratories is caused by different degrees of In clustering.

DOI: 10.1103/PhysRevB.80.075202 PACS number(s): 71.15.Mb, 71.20.Nr, 71.22.+i, 78.55.Cr

I. INTRODUCTION

Semiconducting nitride alloys containing indium, such as $In_xGa_{1-x}N$, $In_xAl_{1-x}N$, and $In_xGa_yAl_{1-x-y}N$, have recently attracted great interest due to their applications in optoelectronics. $In_xGa_{1-x}N$ is used for the construction of green-blue-violet light emitting diodes (LEDs) and blue-violet laser diodes (LDs). Furthermore, $In_xGa_{1-x}N$-based solar cells and detectors operating in the short-wavelength range have been constructed in several laboratories. Similar applications are found for $In_xAl_{1-x}N$ with the advantage that its direct gap (E_g) covers the range from 0.7 (InN) (Ref. 1) to 6.1 eV (AlN),[2] which is the widest range of E_g of any semiconductor alloy system. This makes the $In_xAl_{1-x}N$ alloys candidates for optical applications similar to $In_xGa_{1-x}N$, but operating over a wider spectrum from deep UV to far infrared. Many efforts have been directed toward examination of the properties and applications of $In_xAl_{1-x}N$ alloys with $x \approx 0.17$, because this particular composition makes the alloy lattice matched to GaN.

The $In_xGa_yAl_{1-x-y}N$ quaternary alloys are suitable for all the applications mentioned above but, unlike in ternary alloys, the band gap and the lattice constant can be tuned independently. Varying the composition, one can vary E_g and also match the alloy lattice constant to that of GaN, thus reducing the concentration of defects caused by lattice mismatch (misfit dislocations). Moreover, piezoelectric fields can be tuned in a wide range of magnitudes, for example, in InGaAlN/GaN heterostructures. On the other hand, one can fix the band gap of the alloy to match that of GaN or any other desired values and vary the alloy composition to improve the structural, the optical, and the electronic properties.

In-containing nitride alloys are particularly useful in applications due to the specific role of indium. Addition of In, even in small amounts, to nitride compounds leads to an enhancement of light emission intensity in LEDs and LDs, as shown for $In_xGa_{1-x}N$ and $In_xAl_{1-x}N$ in comparison with GaN and AlN in Ref. 3. Also, in $In_xGa_yAl_{1-x-y}N$ quaternary alloys it has been demonstrated experimentally that the photoluminescence intensity is strongly enhanced compared to that of $Al_xGa_{1-x}N$ with comparable Al concentration.[4] Many attempts were made to explain the phenomena of light emission enhancement when indium atoms are incorporated into the active nitride layers of LEDs or LDs,[5–7] with the most popular being a model proposed by Chichibu *et al.*[5] In this model In clustering leads to potential fluctuations limiting nonradiative recombination of carriers by inhibiting their diffusion from regions of locally reduced band gap to nonradiative recombination centers, such as dislocations. However, the microscopic description of the phenomena related to In clustering is still far from satisfactory. All this makes the nitride alloys with In particularly interesting also from a basic research point of view. Recent progress in the growth of high-quality InN and In-containing alloys has enabled detailed investigation of basic properties of these materials. The compositional instability in wurtzite $In_xGa_{1-x}N$ was studied recently by Ganchenkova *et al.*[8] who demonstrated a high sensitivity of the decomposition to relatively small variations in the cation interaction energies.

The most important parameter of the semiconductor alloy system is the band gap and its composition dependence characterized by the band-gap bowing parameter b, which generally is concentration dependent and defined through

$$E_g(x) = xE_g^{InN} + (1-x)E_g^{GaN} - x(1-x)b(x). \quad (1)$$

Thus $b(x)$ measures the deviation from linear dependence of the band gap on x (Vegard's law). The experimental data indicate that in the case of nitride alloys containing In the bowing parameter is much larger than in "normal" alloys (such as $Al_xGa_{1-x}N$ or $Al_xGa_{1-x}As$), being for $In_xAl_{1-x}N$

 ©2009 The American Physical Society

equal to about 6 eV,[9] and for $In_xGa_{1-x}N$, ranging from 1.43 (Ref. 10) and 1.6 (Ref. 11) to 2.8 eV.[12]

Indium clustering effects and their possible influence on the band structure of nitride alloys containing In, as well as reported significant bowings of E_g for these compounds, motivated the present work. Preliminary calculations[13] for $In_xGa_{1-x}N$ and $In_xAl_{1-x}N$ ternary alloys demonstrated that the band gaps indeed exhibit significant bowing, particularly large when the In atoms cluster.

We analyze the variation in band gaps with indium concentration in $In_xGa_{1-x}N$ and $In_xAl_{1-x}N$ alloys for a wide range of x. Special emphasis is put on the effects of In clustering. We simulate this by supercell calculations for different arrangements of the In atoms. We found that the band gaps indeed exhibit large bowing, and the deviation from Vegard's law is particularly large when the In atoms cluster. Furthermore, the effects are more pronounced in the $In_xAl_{1-x}N$ alloys than in $In_xGa_{1-x}N$, probably due to the larger size difference between In and Al atoms than between In and Ga. Calculations performed for selected sets of quaternary alloys $In_xGa_{1-y}Al_{1-x-y}N$ confirm the strong dependence of the band gap on how the indium atoms are distributed.

The effects of atomic clustering on the optical properties of III-V alloys were already studied by Mäder and Zunger.[14] It was found from their self-consistent pseudopotential calculations that the local clustering reduces the band gaps of $Al_{0.5}Ga_{0.5}As$, $Ga_{0.5}In_{0.5}P$, and $Al_{0.5}In_{0.5}As$ alloys by about 0.1 eV relative to that of the random alloy.

Looking for a possible explanation for the anomalous behavior of E_g, we examine the total valence-band (VB) density of states (DOS) and the partial contributions to the DOS from the constituents of the alloys. We see a direct relation between an increase in the VB width—caused by hybridization between the N and the In states—and a reduction in the band gap. Investigation of the lattice relaxation effects provides some explanation for the observed phenomena. The effect seems to come from the interaction between In atoms and neighboring N atoms, which is enhanced due to the bonds between In and N atoms being shorter in the alloys exhibiting clustering than in InN itself. A related effect was presented in the work of Bellaiche *et al.*[15] where a nonlinear evolution of the $In_xGa_{1-x}N$ band gap with In content was connected with a strong admixture of In states and a hole localization for very low In concentrations.

The organization of the paper is as follows. The methodology is described in Sec. II, and results for binary alloys are shown. In the next sections our results concerning ternary alloys are presented including the structural parameters (Sec. III), the electronic band structure and its dependence on In concentration and In arrangement (Sec. IV), valence-band density-of-state functions (Sec. V), and the lattice relaxation effects (Sec. VI). Finally, in Sec. VII, results for the quaternary $In_xGa_yAl_{1-x-y}N$ alloy are presented, while Sec. VIII summarizes the present work.

II. METHODOLOGY

The electronic structures of the $In_xAl_{1-x}N$, the $In_xGa_{1-x}N$, and the $In_xGa_yAl_{1-x-y}N$ alloys have been analyzed by self-consistent calculations in a supercell model. The indium concentrations, $x=0.12$, 0.19, 0.25, 0.38, 0.50, 0.56, 0.62, 0.75, and 0.87, have been realized by substituting 2, 3, 4, 6, 8, 9, 10, 12, and 14 Al or Ga atoms by In in a 32-atom supercell. For $In_xGa_yAl_{1-x-y}N$ quaternary alloys, we discuss the results for the values of $y=0.19$, 0.38, and 0.62. Different atomic arrangements have been investigated for a given x, by either distributing the In atoms as uniformly as possible over the supercell or by clustering the In atoms together in a small part of the supercell.

Approaches based on the local-density approximation (LDA) to density-functional theory, with the Perdew-Zunger parametrization[16] of the Ceperley-Alder exchange correlation,[17] were used. The calculations were performed in two steps, applying two different computational schemes. In the first step the atomic coordinates in the supercell were determined by minimization of the Hellmann-Feynmann forces for a given distribution of indium atoms. For this task we used pseudopotentials as implemented in the Vienna *ab initio* simulation package (VASP).[18] A cutoff energy of 30 Ry for the plane-wave basis set was sufficient to obtain converged results. The k-space integrations were performed by summing over a $3\times3\times3$ mesh of Monkhorst-Pack special points.[19]

Subsequently, in the second step of calculations, the band structure was obtained including a semiempirical correction for the well-established deficiency of LDA in predicting semiconductor gaps. For this we used the linear-muffin-tin-orbital (LMTO) method[20] in a full-potential version.[21] The semicore cation d states of Ga($3d$) and In($4d$) were included as local orbitals.[22] The calculations were performed for the wurtzite crystal structure, which is the structure of the nitride semiconductors and their alloys at ambient pressure. The supercell is generated by doubling the wurtzite unit cell in three directions. The supercell contains 32 atoms, while 32 additional "empty" muffin-tin spheres were included in the interstitial region for the sake of accurate interpolation of the charge density in the entire volume. We used equal radii of the atomic muffin-tin spheres, slightly less than touching to allow for relaxation. Further details of the LDA-LMTO calculations are given elsewhere.[23,24]

The LDA underestimates the band gaps in semiconductors, and it is necessary to correct for this so-called "LDA error" since we specifically wish to discuss variations in the gaps with composition. Further, since we consider supercells with relatively many atoms, a simple correction scheme was chosen. On the other hand, a correction procedure is needed which not only corrects the fundamental gap, but also the dispersion of the lowest conduction band (CB) and the values of the gaps at other points of the Brillouin zone. Thus, a rigid shift of the unoccupied bands ("scissor operator") is not optimal since it does not change the dispersion of the CB. Therefore, a slightly more advanced correction procedure (LDA+C) has been applied in the present work, introducing at the sites of the atoms, additional external potentials of the form[24]

$$V(r) = V_0\left(\frac{r_0}{r}\right)\exp\left[-\left(\frac{r}{r_0}\right)^2\right], \tag{2}$$

where V_0 and r_0 are adjustable parameters. V_0 is chosen to be very large, and the range parameter r_0 be small. In this way

the potentials become sharply peaked at the nuclear positions, and they produce "artificial Darwin shifts," i.e., they push s states, which have nonzero density at the nuclei ($r=0$) upward in energy. In compound semiconductors different parameters in Eq. (2) are chosen at anion and cation sites. For further flexibility in the adjustment of the lowest CB, we supplement with a constant (r-independent) potential shift V_e at the empty spheres.

The correcting potentials are transferable[24,25] in the sense that they can be determined for binary compounds and subsequently be applied, with unaltered parameters, to systems where the two compounds are combined, as in alloys, superlattices, and heterojunctions.[26] In the present work the parameters were determined for GaN, InN, and AlN by adjusting to experimental gap values and subsequently applied to the $In_xGa_{1-x}N$ and $In_xAl_{1-x}N$ and the $In_xGa_{1-y}Al_{1-x-y}N$ systems. They were kept unchanged while the composition and the volume were varied. This *ad hoc* method for correcting the LDA band-gap errors was developed in the context of LMTO calculations and was extensively used in LMTO (Refs. 23–28) or linear augmented plane-wave calculations.[29,30] Recently, it has also been applied to a pseudopotential framework.[31]

The adjustment procedure requires knowledge of experimental values of gaps in the binaries, InN, GaN, and AlN. Our optimized values of the adjusting parameters are the following: $V_0(\mathrm{In})=V_0(\mathrm{N})=0$, $V_0(\mathrm{Ga})=900$ Ry, and $V_0(\mathrm{Al})=990$ Ry, at the atomic sites with the range parameter set to $r_0=0.015$ a.u. for all atoms. At all the empty spheres we have applied the shift $V_e=0.60$ Ry. It should be noted that a unique set of parameters does not exist and that their values, in particular for the E sites, depend sensitively on the choice of MT sphere radii.

In Table I the calculated (LDA+C) band gaps are compared to the corresponding experimental values and other theoretical results. For InN the adjustment exploited the recent experimental values for the zone center gap being in the range of 0.6–0.7 eV,[32–35] as well as the results of spectroscopic ellipsometry on molecular beam epitaxy (MBE) grown InN films,[36] following the assignments made in Ref. 37. The comparison is made to other experiments[38,39] and to the recent calculations of Ref. 40, using the G_0W_0 approximation to many-body perturbation theory, LDA calculations,[41] "quasiparticle self-consistent GW" calculations,[42] and to LDA calculations in Ref 43. It is worth to mention that our results for InN are slightly different from those given in our previous paper[44] on the band structure of InN. The reason is that in the present work, the adjustment is made not only for InN, but simultaneously for all the binary nitrides considered, with the same values of the adjusting parameters for the nitrogen and empty spheres. For GaN and AlN the adjustment is made using the experimental values from Refs. 38, 45, and 46 and the results are also compared to the same calculations as for InN (Refs. 40, 42, and 43) and to the GW calculations by Rubio *et al.*[47]

TABLE I. The calculated (LDA+C) band gaps in comparison to experimental values and other theoretical results for the binary compounds.

$v\rightarrow c$	LDA+C	Experiment	Other calculations
InN			
Γ_6-Γ_1	0.69	0.65,[a] 0.63,[b] 0.69[c,d]	0.75,[e] 0.69,[f] 0.72,[g] 1.04,[h] 0.65[i]
Γ_5-Γ_6	9.14	8.8,[j] 8.9[k]	10.16,[l] 8.66[i]
M_4-M_1	5.11	5.35,[m] 5.38[m]	5.64,[e] 5.96,[g] 6.56,[h] 5.46[i]
L_1-L_1	5.82	6.05[m]	6.09,[e] 6.00,[h] 5.87[i]
M_3-M_3	8.16	7.87,[m] 7.63[m]	7.94,[e] 7.34,[g] 7.84,[h] 7.78[i]
M_4-M_3	7.52	7.3[j]	6.71[l]
GaN			
Γ_6-Γ_1	3.56	3.44,[n] 3.50[n]	3.47,[l] 3.5,[o] 3.24[f]
K_3-K_2	9.67	9.0[n]	8.54,[l] 9.8[o]
M_4-M_1	7.44	7.0[n]	6.07,[l] 7.6[o]
M_4-M_1	7.48	7.05[j]	7.68,[l] 8.5[o]
AlN			
Γ_6-Γ_1	6.00	6.1[p]	6.47,[f] 6.11,[l] 5.8,[o] 6.76[h]
Γ_5-Γ_3	8.47	8.02[q]	8.95,[l] 9.4[o]
Γ_5-Γ_6	12.37	14.00[q]	12.99,[l] 14.0[o]
H_3-H_3	9.32	10.39[q]	10.10,[l] 10.5[o]

[a]Reference 32.
[b]Reference 33.
[c]Reference 34.
[d]Reference 35.
[e]Reference 37.
[f]Reference 40.
[g]Reference 41.
[h]Reference 42.
[i]Reference 44.
[j]Reference 38.
[k]Reference 39.
[l]Reference 43.
[m]Reference 36.
[n]Reference 45.
[o]Reference 47.
[p]Reference 2.
[q]Reference 46.

III. STRUCTURAL PARAMETERS

Calculations of the lattice parameters of $In_xGa_{1-x}N$ and $In_xAl_{1-x}N$ have been performed for several values of In content x. Two types of alloys have been considered, i.e., (i) alloys with uniformly distributed In atoms in the 32-atom supercell and (ii) alloys with all In atoms clustered. In addition, for the Al alloy, some "intermediate" arrangements were treated. For each value of x, the structures of $In_xGa_{1-x}N$ and $In_xAl_{1-x}N$ have been optimized by minimization of the total energy with respect to atomic coordinates and a and c parameters of the supercell.

The results are summarized in Figs. 1(a) and 1(b), where the lattice parameters a and c are plotted for $In_xGa_{1-x}N$ and $In_xAl_{1-x}N$ as functions of x. In the case of uniformly distributed In atoms the dependence of a and c on x is almost linear, whereas in the alloys with clustered In atoms the deviations from linearity are somewhat larger. In particular, the calculated c lattice constants vs x are larger for both clustered alloys [Fig. 1(b)]. Note however, that the results of the latter calculations may depend on the choice of structure of the clusters. The results shown here are for the "most clustered case" (see Sec. IV). Our results for $In_xGa_{1-x}N$ are in a good agreement with Ref. 48, where also small deviations of the theoretical lattice parameters from the Vegard's law prediction were reported (for the uniform case).

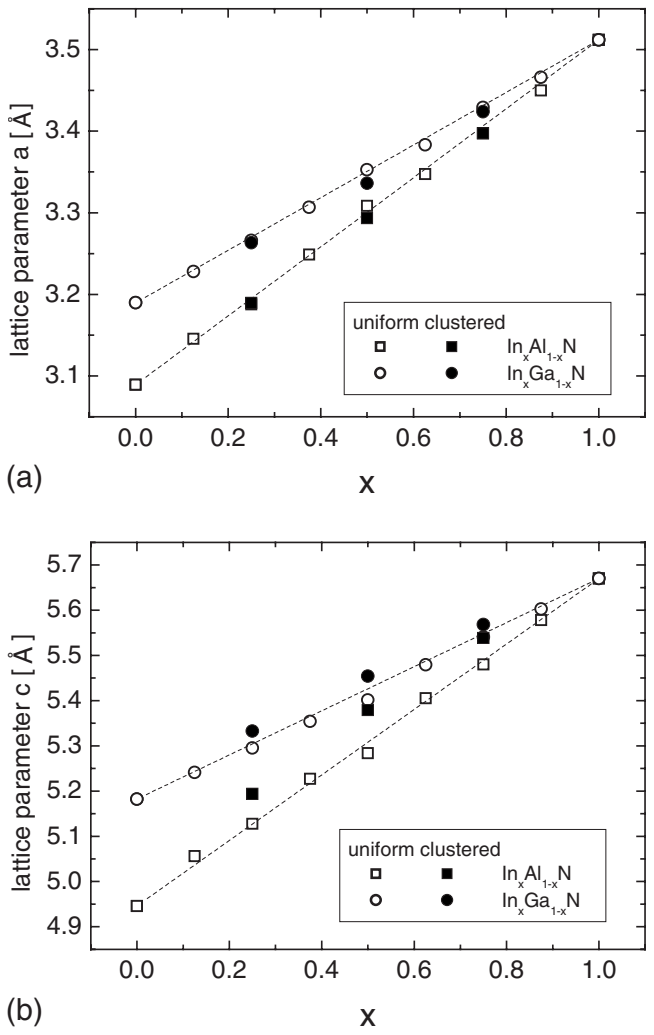

FIG. 1. Theoretical equilibrium lattice parameters (a) a and (b) c for $In_xGa_{1-x}N$ (circles) and $In_xAl_{1-x}N$ (squares) as functions of indium concentration x. Calculations are performed for two models of In distribution in the supercell: uniform (open symbols) and clustered (filled symbols). The dashed lines are linear interpolations between the end points.

In order to check the accuracy of computations, we have performed additional calculations of the structural parameters for the binary compounds using a four-atom unit cell. In this case, the total-energy calculations have been performed using $11\times11\times7$ Monkhorst-Pack k-space grid and the kinetic-energy cutoff for the plane-wave basis set E_{cutoff}=800 eV. The values obtained for a and c using a four-atom unit cell are in excellent agreement with the results obtained using the 32-atom supercell.

IV. BAND-GAP BOWINGS OF TERNARIES

Figure 2 shows the calculated and the measured energy gaps E_g of $In_xAl_{1-x}N$ as functions of x. The solid lines represent fits to the calculated gap variations and illustrate the bowing for two cases: In atoms distributed uniformly in the supercell and In atoms clustered. Generally, the clustering can be realized in different ways as was already discussed in

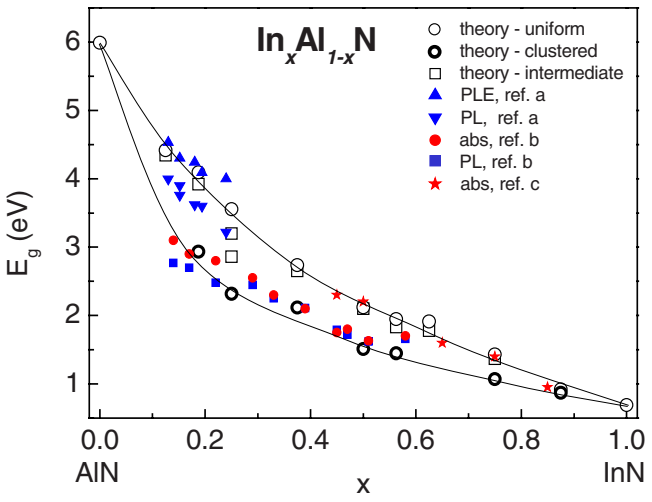

FIG. 2. (Color online) Energy gap of $In_xAl_{1-x}N$ as a function of composition x. Calculations (open circles) are shown for both the uniform (thin circles), most clustered (thick circles), and some intermediate In distribution models (squares). Solid lines are spline fits to the calculated values (uniform and most clustered cases). Measured optical energy gaps of $In_xAl_{1-x}N$ are also marked from a: Ref. 9, b: Ref. 49, and c: Ref. 50.

Ref. 8, and there is no unique definition of "most" or "least" uniform configuration for a given x. As an example, let us consider the case of four In atoms in the 32-atom supercell (x=0.25). A possible optimum clustered configuration would have every fourth cation hexagonal layer consisting entirely of In atoms (case 1). A second possibility is to have four In atoms as neighbors of the same N atom (case 2). In contrast, the uniform distribution of In atoms would have In as one out of four cations in each hexagonal layer (to each N atom belong one In and three Al neighbors). The calculated band gap is largest for the uniform distribution (highest circle in Fig. 2) and lowest in the former "clustering" scenario (case 1), corresponding to the lowest thick circle in Fig. 2 for x =0.25. The latter clustering scenario (case 2) corresponds to the lower square, while the upper square corresponds to an intermediate In distribution.

From the figure it is clear that the band-gap bowing is very large, especially in the clustered case, and composition dependent, i.e., the $E_g(x)$ function deviates from a pure parabolic behavior. The bowing parameter ranges for the uniform case from 2.1 to 6.2 eV, being equal to 4.4 eV for x=0.5. In the clustered case the bowing is almost twice as large, ranging from 3.9 to 14 eV, with a value of 8.6 eV for x=0.5. The most recently reported experimental value of the bowing parameter of $In_xAl_{1-x}N$ of $\approx$6 eV (for $0.13<x<0.24$)[9] falls in between our calculated values for the two In configuration scenarios investigated.

Composition fluctuation induced variations in band gaps (Γ-Γ and Γ-X) in *cubic* $In_xAl_{1-x}N$ were calculated by Teles *et al.*[49] They derived average gaps (E_g) and the rms deviation (ΔE_g) vs x. ΔE_g attains for Γ-Γ particularly large values, reaching a maximum of 1.5 eV near x=0.4. Thus, for Γ-Γ the bowing parameter for the average (E_g) and the minimum ($E_g-\Delta E_g$) gaps are very different in magnitude, b=1.32 and 6.6 eV, respectively. The calculations of Ref. 49 were made

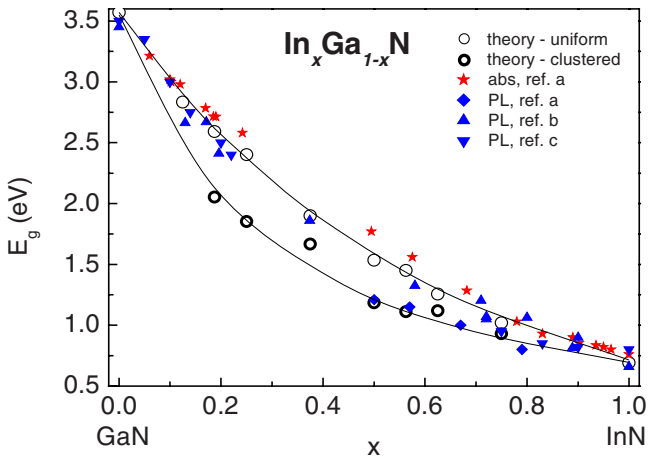

FIG. 3. (Color online) Energy gap of $In_xGa_{1-x}N$ as a function of composition x. Calculations are shown for both the uniform (thin circles) and clustered (thick circles) In distribution models. Solid lines are spline fits to the calculated values. Measured optical energy gaps of $In_xGa_{1-x}N$ are also marked from a: Ref. 10, b: Ref. 11, and c: Ref. 12.

for the zinc-blende structure, but nevertheless the bowing parameters agree reasonably well with our values for the "uniform" (2.1 eV) and "clustered" case (6.2 eV), respectively.

The energy-gap bowing found in $In_xGa_{1-x}N$ is weaker (see Fig. 3), and also the difference between the uniform and the clustered cases is less pronounced. The gap bowing ranges for the uniform case from 1.7 (large x) to 2.8 eV (small x), being equal to 2.1 eV for $x=0.5$. In the clustered case the bowing is significantly larger, ranging from 2.5 (large x) to 6.5 eV (small x), and equal to 3.9 eV for $x=0.5$. The experimental $In_xGa_{1-x}N$ bowing parameter is still a subject of discussion. Experimental values found in the literature vary between[10] 1.43 and 1.6 eV,[11] while recently a considerably larger value was reported: 2.8 eV.[12] The theoretical values range from 1.37 (Ref. 50) and 1.89 (Ref. 51) to 5.14 eV.[52] The composition-dependent bowing was found by Teles *et al.*[52] for cubic $In_xGa_{1-x}N$. In analogy with their study of cubic $In_xAl_{1-x}N$ they found small bowing parameter for the average band gap, $b=(0.74-0.10x)$ eV, and much larger bowing, $b=(5.14-2.59x)$ eV, for the minimum gap.

The band-gap values obtained in the present work differ slightly from those of Ref. 13. The differences are mainly due to the linear x dependence of the structural parameters assumed in the preliminary calculations, an approximation which was sufficient for prediction of trends. In order to obtain a quantitative description, here, we perform full structural optimizations. Further, a larger number of x values are considered in the present work. Consequently, the present Figs. 2 and 3 represent more accurate results than the corresponding Figs. 1 and 2 of Ref. 13. Also, the values of the gap bowings, which are the central results of this work, differ significantly (by up to 50%) from the preliminary calculations.

The calculated variations in the band gap with x in $In_xAl_{1-x}N$ and $In_xGa_{1-x}N$ are compared in Figs. 2 and 3, respectively, with experimental absorption[10,53,54] and photoluminescence[9,11,12,53] data. We observe that the experimental data are scattered, but generally they fall between our two curves corresponding to uniform and clustered In configurations.

The energy difference, ΔE_{uc}, between the band gap in the uniform and clustered case is largest for $x=0.25$, in both alloys, $\Delta E_{uc}=1.2$ eV in $In_{0.25}Al_{0.75}N$ and $\Delta E_{uc}=0.5$ eV in $In_{0.25}Ga_{0.75}N$. The large magnitude of ΔE_{uc} found here for nitrides can be compared with the results obtained by Mäder and Zunger[14] for more traditional semiconductor alloys. In particular, their biggest reduction in the band gap (0.13 eV) obtained for the $In_{0.5}Ga_{0.5}P$ is considerably smaller than our result for $In_{0.5}Ga_{0.5}N$ ($\Delta E_{uc}=0.35$ eV), showing the significant role of nitrogen. It demonstrates that the clustering effects are more pronounced in nitrides than in other III-V alloys.

It is worthwhile to comment on material-related as well as experimental issues causing limitations in the accuracy of the band-gap determination in semiconductor alloys. It concerns in particular materials with constituent cations (or anions) differing significantly in ionic radii. $In_xGa_{1-x}N$ and even to higher extent $In_xAl_{1-x}N$ represent this situation. The most commonly used techniques for studies of E_g are light absorption and light emission. The latter process is usually examined in photoluminescence experiments. Both methods carry information about E_g and its dependence on chemical composition in the alloys, provided that these effects originate from interband transitions, as they manifest themselves in the dielectric function [$\varepsilon_2(\omega)$, for example]. To some extent a theoretical analysis can be made using the joint density of states. However, in the case of light absorption, a necessary condition for the availability of the empty state in the CB makes this effect very sensitive to the Fermi-level position, and hence the concentration of free carriers. The Burstein-Moss effect describes this phenomenon and leads to a blueshift of the assigned E_g in n-type material. Another effect influencing E_g in the opposite direction is caused by band-gap renormalization. Photoluminescence is particularly sensitive to the local fluctuations of the CB and the VB bottom and top, respectively, originating from a nonuniform distribution of the alloy constituents and/or strain. Locally, an increased concentration of In induces a decrease in E_g, which is likely to be seen in luminescence experiments, but less important for absorption measurements. The well-known Stokes shift is a direct consequence of such a situation. One expects, and experiments confirm this, that with increasing x in $In_xGa_{1-x}N$ and $In_xAl_{1-x}N$ the magnitude of the Stokes shift increases to a maximum around $x=0.5$. In In-containing nitride alloys, the Stokes shift can approach few hundreds of meV. Of course, the magnitude of the Stokes shift depends on the scale of the fluctuating potential, which again depends on the extent to which In clustering occurs, and on the spatial extent of In nanoclusters forming. This dependence is however not well understood. The influence of strain leads to roughly parallel shifts of the CB and the VB edges leading to less pronounced effects with respect to the experimental determination of E_g.

With all the above reservations, one has to be careful in extracting E_g from experiments independently of the method used for its determination. Inspection of Figs. 2 and 3, which

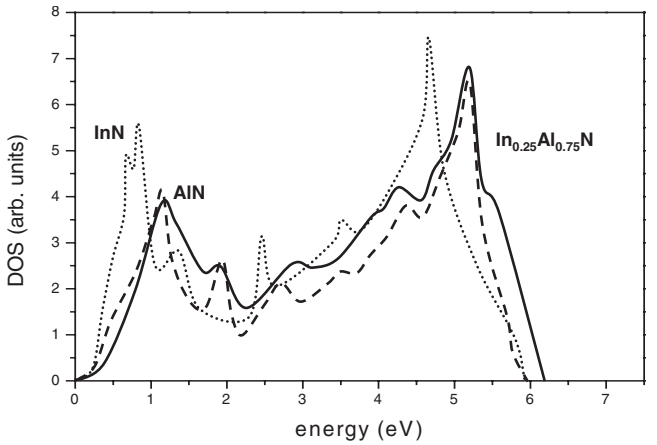

FIG. 4. Valence-band density of states for InN (dotted line), AlN (dashed line), and $In_{0.25}Al_{0.75}N$ (solid line) for the case of a uniform In distribution.

give a collection of experimental data on E_g versus x in $In_xAl_{1-x}N$ and $In_xGa_{1-x}N$, shows that absorptionlike data do not necessarily exhibit larger E_g value than photoluminescence results. This observation suggests that In clustering inherent to the particular epitaxial growth procedure or technique is a likely cause for the significant scatter of E_g values for a given In concentration, and hence for the reported variations in the value of the bowing parameter.

V. VALENCE-BAND DENSITY OF STATES

Looking for an explanation of the peculiar behavior of the band gaps in In-containing nitride alloys as functions of In composition and clustering, we investigate the DOS as a function of indium concentration. Analyzing the band structures and the DOS up to 75% indium, we found no states in the gap. Also, the In contribution to the lower part of the CB is negligible. Tentatively, it is suggested that this peculiar behavior is related to In-induced states at the top of the VB.[55] To check this hypothesis we performed a detailed analysis of the VB DOS for one particular case, namely, $In_xAl_{1-x}N$, with $x=0.25$, for both uniform and clustered In arrangements, in which case we observe the largest band-gap difference ($\Delta E_{uc} \approx 1.2$ eV) between the two arrangements of In atoms. Figure 4 shows the VB DOS as calculated for $In_xAl_{1-x}N$ for $x=1$, 0, and 0.25, respectively. $In_{0.25}Al_{0.75}N$ is shown in the case of a uniform In distribution. In all cases the bottom of the VB (N-2*s* band) is used as the energy reference level.

Figure 4 shows that in the uniform case the VB top for $In_{0.25}Al_{0.75}N$ has a similar shape as for the binaries, but the VB width is slightly larger. The picture is quite different in the clustered case, which is illustrated in Fig. 5. The VB DOS for $In_{0.25}Al_{0.75}N$ in this case has a peculiar shape at the top and consequently a width, which is roughly 1 eV larger than that of the corresponding uniform alloy (Fig. 4). The 1 eV expansion of the VB width in the clustered case is similar to the difference between the band gaps of uniform and clustered $In_{0.25}Al_{0.75}N$ ($\Delta E_{uc}=1.2$ eV), leading to the conclusion that the decrease in the band gap upon clustering comes mainly from the ensuing VB width expansion.

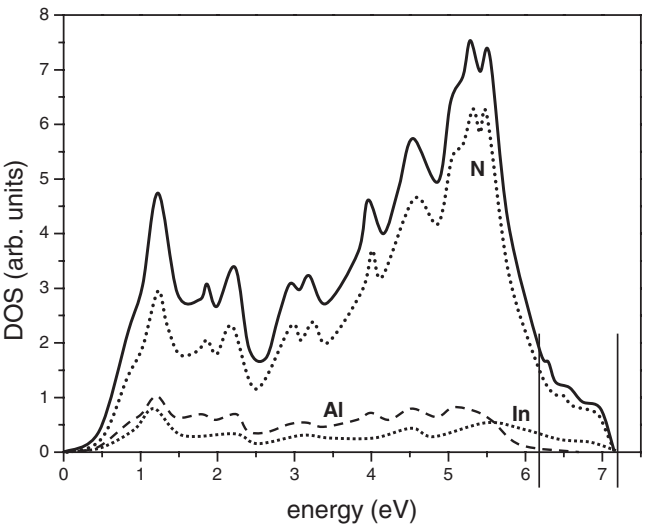

FIG. 5. Valence-band density of states for $In_{0.25}Al_{0.75}N$ for the case of a clustered In distribution (case 1, see text). The decomposition into Al (dashed line), In (short dashed line), and N (dotted line) partial DOS is shown. The region of interest is the top ~1 eV of the valence band, marked with vertical bars.

Looking next for the microscopic explanation for the VB width increase in the clustered case, we analyzed the partial DOS to find which atomic states are responsible for this effect. The main contribution to the VB DOS comes from N(p) states, as illustrated in the Fig. 5. On the other hand, in the clustered case we deal with two types of nitrogen atoms: those which are nearest neighbors only of Al atoms (N1) and those which are neighbors of In atoms (N2), and we may decompose the N contribution to the total DOS into contributions from N1 and N2 atoms. Partial DOSs corresponding to N1 and N2 atoms are presented on Fig. 6, and they are seen to give quite different contributions to the total VB DOS; in fact only N2 states are responsible for the particular

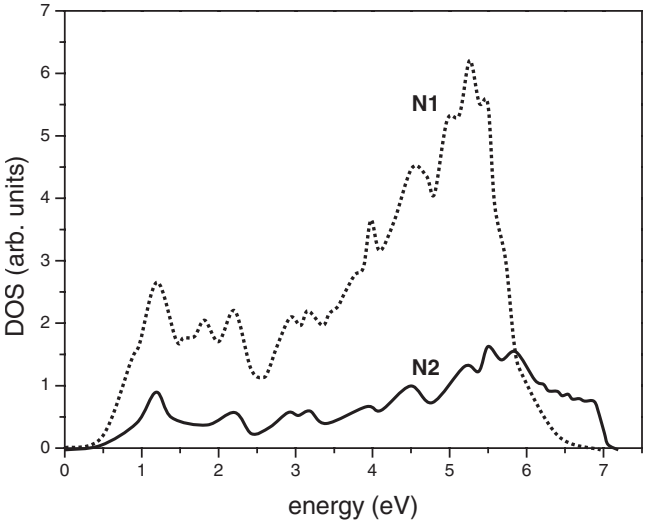

FIG. 6. Partial nitrogen band density of states for $In_{0.25}Al_{0.75}N$ for the same case as in Fig. 5; however, it is further decomposed into In nearest neighbors N2 (solid line) and other nitrogen N1 (dotted line) contributions.

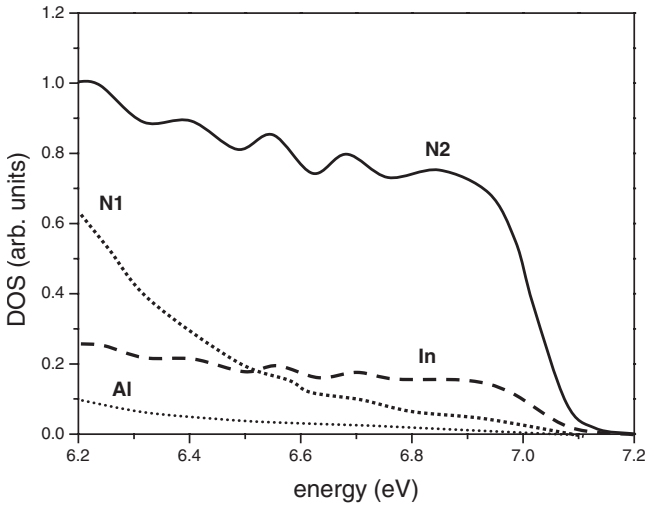

FIG. 7. Same as Figs. 5 and 6, but enlarged around the valence-band top.

shape of the top of the VB DOS in the clustered alloy. Figure 7 shows an enlarged picture of the region around the VB top. It follows that N2 states interacting with In(p,d) states are dramatically pushed out from the VB top changing the shape of the VB edge.

A similar analysis performed for $In_{0.25}Ga_{0.75}N$ is illustrated in Figs. 8 and 9. Comparing the uniform and the clustered $In_{0.25}Ga_{0.75}N$ alloys, we observe an expansion of the VB width of about 0.45 eV, which again corresponds to the difference between the uniform and the clustered band gaps of $In_{0.25}Ga_{0.75}N$ (ΔE_{uc}=0.5 eV). It agrees with the conclusion drawn from the analysis of $In_xAl_{1-x}N$, i.e., that the decrease in the band gap comes mainly from the VB width expansion. Consequently, another question arises: why do the states of indium atoms interact so strongly with the N2 atoms in the case of the clustered alloy? To answer this question, we performed analysis of the lattice relaxation for the alloys in the two cases, uniform and clustered In arrangements, to be discussed in the next section.

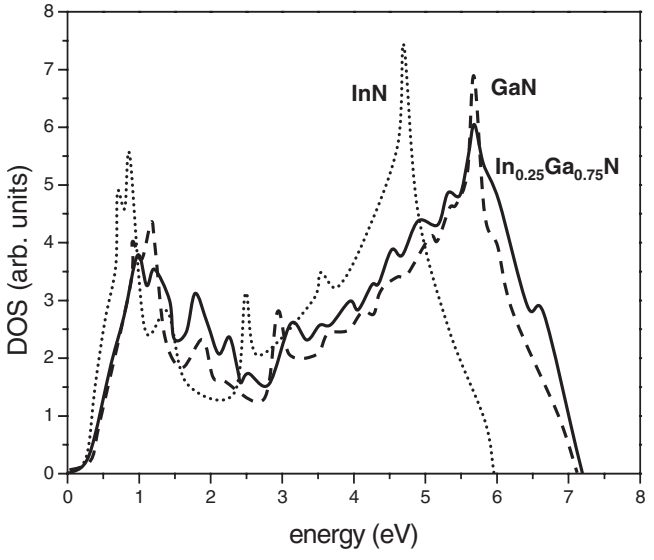

FIG. 8. Valence-band density of states for InN (dotted line), GaN (dashed line), and $In_{0.25}Ga_{0.75}N$ (solid line) for the case of a uniform In distribution.

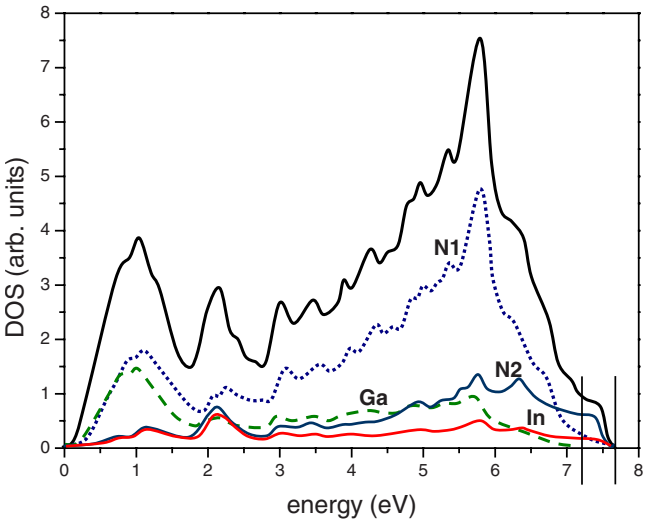

FIG. 9. (Color online) Valence-band density of states for $In_{0.25}Ga_{0.75}N$ for the case of a clustered In distribution (case 1, see text). The decomposition into Ga (dashed line), In (lowest line), N1 (short dashed line), and N2 (line) partial DOS is shown. The region of interest is the top ~0.45 eV of the valence band, marked with vertical bars.

VI. LATTICE RELAXATIONS

In Fig. 10 the bond lengths (in Å) of the binary compounds AlN, GaN, and InN are schematically illustrated. In Fig. 11 the bond lengths are shown for the $In_{0.25}Al_{0.75}N$ and the $In_{0.25}Ga_{0.75}N$ alloys in the uniform and the clustered indium arrangements.

For the $In_{0.25}Ga_{0.75}N$ alloy we compare two clustered arrangements, as has already been discussed in Sec. IV. The largest band-gap reduction was found for the situation where every fourth cation hexagonal layer is made of In (case 1), while the band gap was slightly larger in the case where four In atoms have a common N neighbor (case 2). The relaxed bond lengths for the two cases are illustrated in Fig. 11.

In the uniform $In_xAl_{1-x}N$ alloy, we observe almost no changes in bond lengths going from the binaries to $In_{0.25}Al_{0.75}N$, whereas in the clustered alloy (case 1) the In-N2 bonds are 5% shorter (2.05 Å) than those in pure InN

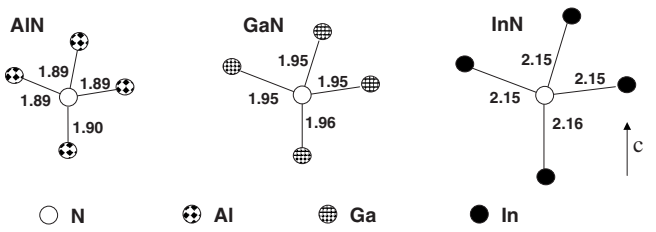

FIG. 10. Schematic arrangement of atoms for InN, AlN, and GaN. Nitrogen is in the middle and its four nearest-neighbor cations are shown. The bond lengths (in Å) are indicated.

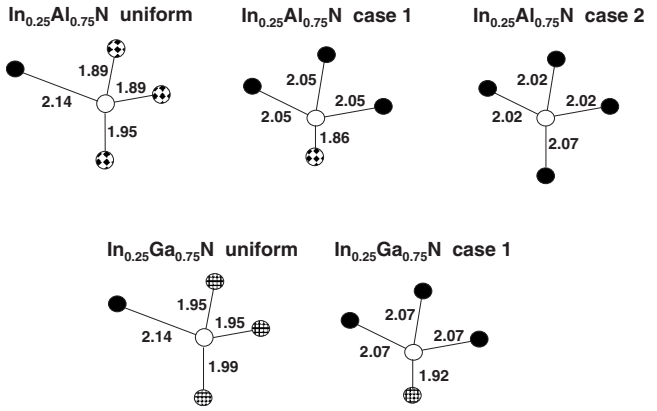

FIG. 11. Schematic arrangement of atoms for $In_{0.25}Al_{0.75}N$ and $In_{0.25}Ga_{0.75}N$ in the uniform and clustered cases (see text for discussion). Symbols are defined in Fig. 10. Nitrogen is in the middle, and only the configuration around nitrogen atoms with largest number of In atoms as nearest neighbor is shown. The calculated equilibrium bond lengths (in Å) are indicated

(2.15 Å), and also the Al-N2 bond (1.86 Å) is shorter than in the host AlN. Shorter In-N2 bonds reflect that the interaction between indium and nitrogen atoms is stronger than in pure InN, which leads to an increased hybridization between In(p,d) and N2(p) states. As a result, the N2(p) states are pushed up, changing the VB edge shape and its width. In the clustered case 2, we observe even more pronounced shortening of the In-N2 bonds (2.02 Å), but only one N2 atom experiences such short bonds (other In-N bonds in this case are between 2.07 and 2.15 Å). In the clustered case 1 short In-N2 bonds exist for all four N2 atoms.

In $In_xGa_{1-x}N$ very similar effects occur, but they are smaller: there are almost no changes in bond lengths going from the binaries to the uniformly distributed $In_{0.25}Ga_{0.75}N$ alloy, but the In-N2 bonds are shorter (2.07 Å) in the clustered alloy than in InN itself (2.15 Å). Smaller difference in bond lengths between GaN and InN than between InN and AlN are in agreement with the fact that all the effects connected with In clustering are more pronounced in the $In_xAl_{1-x}N$ alloys than in $In_xGa_{1-x}N$. Studying the atomic relaxation pattern around an In atom in InGaN, Ganchenkova *et al.*[8] found the values of the In-N bond lengths (2.08 and 2.10 Å) lying somewhere between our values for the uniform and the clustered cases.

VII. QUATERNARY ALLOYS

We performed studies of quaternary $In_xGa_yAl_{1-x-y}N$ alloys along similar lines as were discussed for the ternary alloys in the previous sections. First, we consider $In_xGa_yAl_{1-x-y}N$ alloys with a fixed indium content x, and subsequently another set of alloys with fixed Ga concentration y is examined.

In the first case, with the fixed values of $x=0.06$, 0.12, 0.19, 0.25, 0.38, 0.50, and 0.87, the Ga concentration y is varied between 0 and $1-x$. The band-gap bowings for uniform arrangements of In atoms are presented in Fig. 12. The gap bowings for all these alloys are very small, varying between $b=0$ and $b=0.65$. Such an almost linear behavior of the band gap of $In_xGa_yAl_{1-x-y}N$ alloys with fixed content of indium is not surprising, because they are similar to the $Ga_xAl_{1-x}N$ alloy, which exhibits rather small band-gap bowing (typically below 1 eV).[56]

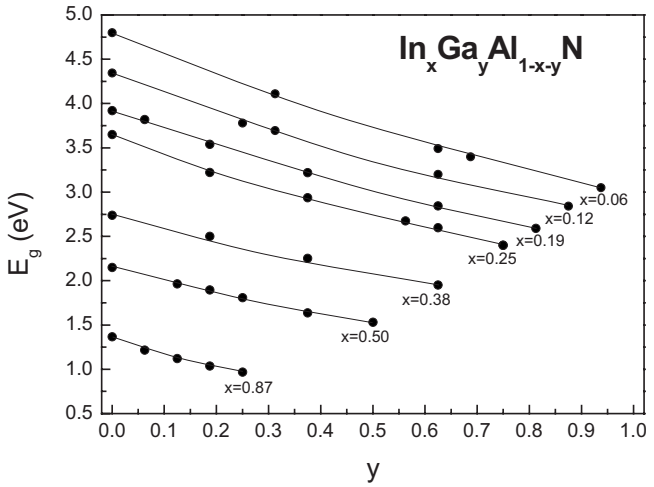

FIG. 12. Energy gaps (in eV) of $In_xGa_yAl_{1-x-y}N$ for a series of x values, as a function of Ga concentration y, for a uniform model of the In distribution. The lines are smooth fits to the calculated points.

For one of the cases presented in Fig. 12, namely, $x=0.19$ (three indium atoms in a 32-atom supercell), we compare in Fig. 13 the band-gap bowing for a uniform arrangement of In with the gap bowing for a clustered arrangement of In atoms. The band-gap bowing going from $In_{0.19}Al_{0.81}N$ to $In_{0.19}Ga_{0.81}N$ is very small in either scenario (b is between 0 and 0.4) and we do not observe larger gap bowing in the clustered arrangement, in contrast to the case where we varied the In content in $In_xAl_{1-x}N$ and $In_xGa_{1-x}N$. More interesting is the large difference between the curves for the two In arrangements, which however is diminished as the Ga content is increased. Starting from the value of ΔE_{uc}

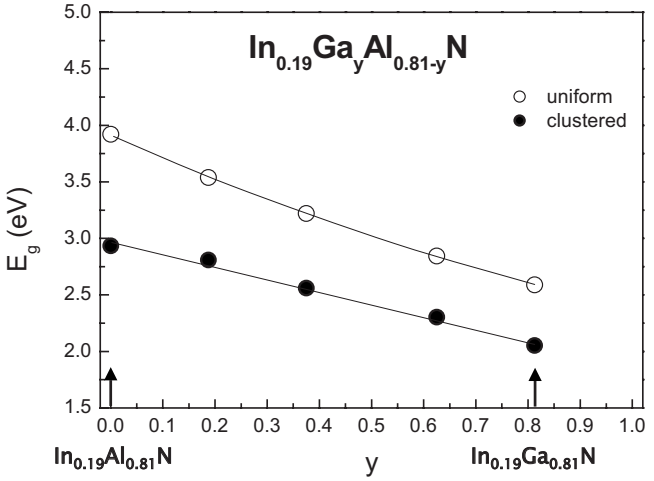

FIG. 13. Energy gaps (in eV) of $In_xGa_yAl_{1-x-y}N$ for $x=0.19$, as a function of Ga concentration y, for uniform (open circles) and clustered (filled circles) model of the In distribution. The lines are smooth fits to the calculated points.

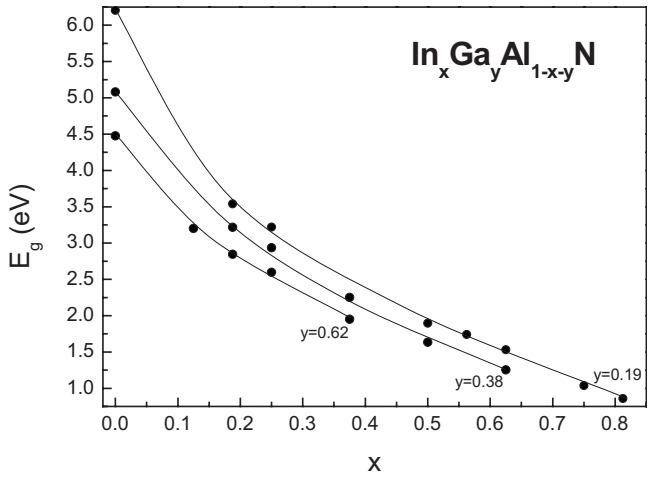

FIG. 14. Energy gaps (in eV) of $In_xGa_yAl_{1-x-y}N$ for a series of y values, as a function of In concentration x, for a uniform In distribution model. The lines are guides to the eyes.

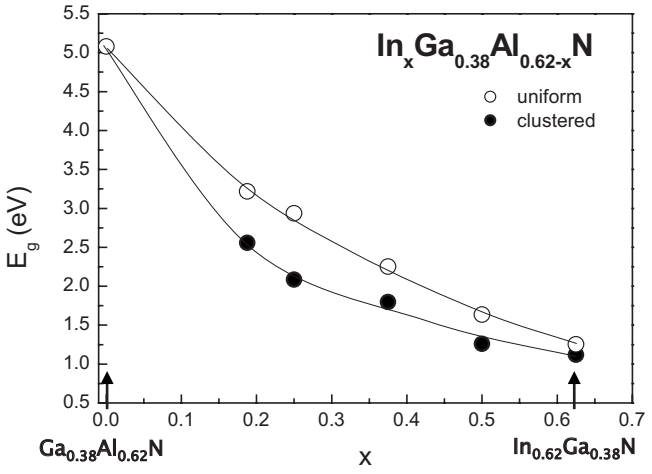

FIG. 15. Energy gaps (in eV) of $In_xGa_yAl_{1-x-y}N$ for $y=0.38$, as a function of In concentration x, for uniform (open circles) and clustered (filled circles) In distribution models. The lines are guides to the eyes.

$=1.2$ eV for $In_{0.19}Al_{0.81}N$, it decreases almost linearly in y to the value $\Delta E_{uc}=0.5$ eV for $In_{0.19}Ga_{0.81}N$.

The situation is quite different when we consider the second set of alloys with fixed Ga concentration y and varying value of indium content x. Figure 14 shows the band-gap bowings for uniform arrangements of In atoms for three values of Ga concentration: $y=0.19$, 0.38, and 0.62, with x changing from 0 to $1-y$. For these alloys we observe large band-gap bowings, being the most pronounced for the smallest Ga concentration, $y=0.19$ (the largest Al concentration). The composition-dependent b ranges in this case from 3.2 to 6.3 eV with 4.3 eV for $x=0.5$. These values are very similar to those obtained for $In_xAl_{1-x}N$ (2.1–6.2, with 4.4 eV for $x=0.5$). Going to larger Ga (smaller Al) concentrations, we have found also smaller gap bowings; about 2.6 eV for $y=0.38$; and about 2.0 eV for $y=0.62$, i.e., these values approach those obtained for $In_xGa_{1-x}N$ ($y=1.0$), 1.7–2.8 eV.

In Fig. 15 we compare the alloy with fixed Ga concentration, $y=0.38$, in uniform and clustered arrangements of In atoms. For this case a significant band-gap bowing is found, being most pronounced in the case of clustered arrangements of In atoms ($b\approx 2.6$ for uniform and $b\approx 4.3$ for clustered alloy), similar to what was found for $In_xAl_{1-x}N$ and $In_xGa_{1-x}N$. The lattice relaxation is also different in the uniform and the clustered cases of the alloy presented on Fig. 15. For $x=0.25$, we have got the shortest In-N bond length equal to 2.11 Å for uniform and 2.06 Å for clustered indium arrangements. The latter value is between the lengths of similar bonds in $In_xAl_{1-x}N$ (2.05 Å) and $In_xGa_{1-x}N$ (2.07 Å) (see Fig. 11).These results demonstrate that strong bowings are also present in quaternary nitride semiconductor alloys, very similar to those found for ternary alloys, especially in the case of clustered alloys when the dependence on indium content is considered.

VIII. SUMMARY

The electronic structures of $In_xGa_{1-x}N$ and $In_xAl_{1-x}N$ were calculated for fully relaxed supercell structures. Both plane-wave pseudopotential and full-potential LMTO methods were used. The band gaps for x varying over the entire range between 0 and 1 were derived and compared to existing experimental data. Significant composition-dependent bowings of the gaps were found. The clustering of In atoms affects the band gap, which become particularly small when the In atoms cluster. The large band-gap bowings calculated in this work correspond well to existing experimental values, which generally fall between the values calculated for the uniform and for the most clustered cases of In arrangements. The effects are more pronounced in $In_xAl_{1-x}N$ than in $In_xGa_{1-x}N$. The largest difference between the band gaps in the clustered and the uniform cases is found for $x\approx 0.25$, where we have obtained $\Delta E_{uc}=1.2$ eV (for $In_{0.25}Al_{0.75}N$) and $\Delta E_{uc}=0.5$ eV (for $In_{0.25}Ga_{0.75}N$).

Results for quaternary alloys, $In_xGa_yAl_{1-x-y}N$, have been presented. The band-gap dependence on cation composition for constant In concentration shows an almost linear behavior between the Al-rich and the Ga-rich limits, whereas a strong band-gap bowing as a function of In content is found for constant Ga concentration.

The unusual decrease in the band gaps with In content is found to stem from the In-induced changes in the states at the VB top. It relates to the increase in the VB width due to (hybridization) admixture of In p and d states into the uppermost valence states. From the detailed analysis of the lattice relaxations, it emerges that the strong interaction of In atoms and neighboring N atoms is related to the shorter bonds between them in the cases representing the In clustering.

The two models for In-atom distributions, uniform and clustered, which we have considered here, represent in a sense extreme limits, and actual samples might be characterized by an intermediate distribution. The scatter in experimental values for band gaps of In-containing nitride alloys may reflect different degrees of clustering of In atoms in samples depending on growth conditions, growth methods, and the substrates including their orientations. It would be interesting to examine whether, in the latter context, nonpolar and semipolar vs polar structures could cause differences.

ACKNOWLEDGMENTS

This work was partially supported by the projects of the Polish Ministry of Higher Education and Science (Contracts No. 1P03B 037 29 and No. NN507 439134, and Scientific Network New Materials development and structure investigation). The Danish Centre for Scientific Computing (DCSC) is gratefully acknowledged for financial support for computing facilities. Additionally, we acknowledge the use of computing facilities at ICM University of Warsaw.

[1] J. Wu, W. Walukiewicz, K. M. Yu, J. W. Ager III, E. E. Haller, H. Lu, W. J. Schaff, Y. Saito, and Y. Nanishi, Appl. Phys. Lett. **80**, 3967 (2002).
[2] I. Vurgaftman and J. R. Meyer, J. Appl. Phys. **94**, 3675 (2003).
[3] S. Nakamura and G. Fasol, *The Blue Laser Diode* (Springer, Berlin, 1997).
[4] C. H. Chen, L. Y. Huang, Y. F. Chen, H. X. Yang, and J. Y. Lin, Appl. Phys. Lett. **80**, 1397 (2002).
[5] S. Chichibu, T. Azuhata, T. Sota, and S. Nakamura, Appl. Phys. Lett. **70**, 2822 (1997).
[6] M. D. McCluskey, L. T. Romano, B. S. Krusor, D. P. Bour, N. M. Johnson, and S. Brennan, Appl. Phys. Lett. **72**, 1730 (1998).
[7] K. P. O'Donnell, R. W. Martin, and P. G. Middleton, Phys. Rev. Lett. **82**, 237 (1999).
[8] M. G. Ganchenkova, V. A. Borodin, K. Laaksonen, and R. M. Nieminen, Phys. Rev. B **77**, 075207 (2008).
[9] K. Wang, R. W. Martin, D. Amabile, P. R. Edwards, S. Hermandez, E. Nogales, K. P. O'Donnel, K. Lorenz, E. Alves, V. Matias, A. Vantomme, D. Wolverson, and I. M. Watson, J. Appl. Phys. **103**, 073510 (2008).
[10] J. Wu, W. Walukiewicz, K. M. Yu, J. W. Ager III, E. E. Haller, H. Lu, and W. J. Schaff, Appl. Phys. Lett. **80**, 4741 (2002).
[11] G. Franssen, I. Gorczyca, T. Suski, A. Kamińska, J. Pereiro, E. Munoz, E. Iliopoulos, A. Georgakilas, S. B. Che, Y. Ishitani, A. Yoshikawa, N. E. Christensen, and A. Svane, J. Appl. Phys. **103**, 033514 (2008).
[12] M. Moret, B. Gil, S. Ruffenach, O. Briot, Ch. Giesen, M. Heuken, S. Rushworth, T. Leese, and M. Succi, J. Cryst. Growth **311**, 2795 (2009).
[13] I. Gorczyca, T. Suski, N. E. Christensen, and A. Svane, Phys. Status Solidi C **6**, S368 (2009).
[14] K. A. Mäder and A. Zunger, Appl. Phys. Lett. **64**, 2882 (1994).
[15] L. Bellaiche, T. Matilla, L.-W. Wang, S.-H. Wei, and A. Zunger, Appl. Phys. Lett. **74**, 1842 (1999).
[16] J. P. Perdew and A. Zunger, Phys. Rev. B **23**, 5048 (1981).
[17] D. M. Ceperley and B. J. Alder, Phys. Rev. Lett. **45**, 566 (1980).
[18] G. Kresse and J. Furthmüller, Comput. Mater. Sci. **6**, 15 (1996).
[19] H. J. Monkhorst and J. D. Pack, Phys. Rev. B **13**, 5188 (1976).
[20] O. K. Andersen, Phys. Rev. B **12**, 3060 (1975).
[21] M. Methfessel, Phys. Rev. B **38**, 1537 (1988); M. Methfessel, C. O. Rodriguez, and O. K. Andersen, *ibid.* **40**, 2009 (1989).
[22] D. Singh, Phys. Rev. B **43**, 6388 (1991).
[23] N. E. Christensen and I. Gorczyca, Phys. Rev. B **50**, 4397 (1994).
[24] N. E. Christensen, Phys. Rev. B **30**, 5753 (1984).
[25] I. Gorczyca, N. E. Christensen, and M. Alouani, Phys. Rev. B **39**, 7705 (1989).
[26] M. Cardona, T. Suemoto, N. E. Christensen, T. Isu, and K. Ploog, Phys. Rev. B **36**, 5906 (1987).
[27] M. Cardona, N. E. Christensen, and G. Fasol, Phys. Rev. B **38**, 1806 (1988).
[28] I. Gorczyca and N. E. Christensen, Solid State Commun. **80**, 335 (1991).
[29] S. H. Wei and A. Zunger, Phys. Rev. B **57**, 8983 (1998); S.-H. Wei, X. Nie, I. G. Batyrev, and S. B. Zhang, *ibid.* **67**, 165209 (2003).
[30] P. Carrier and S.-H. Wei, J. Appl. Phys. **97**, 033707 (2005).
[31] D. Segev, A. Janotti, and C. G. Van de Walle, Phys. Rev. B **75**, 035201 (2007).
[32] V. Yu. Davydov, A. A. Klochikhin, R. P. Seisyan, V. V. Emtsev, S. V. Ivanov, F. Bechstedt, J. Furthmüller, H. Harima, A. V. Mudryi, J. Aderhold, O. Semchinova, and J. Graul, Phys. Status Solidi B **229**, R1 (2002).
[33] S. X. Li, J. Wu, E. E. Haller, W. Walukiewicz, W. Shan, H. Lu, and W. J. Schaff, Appl. Phys. Lett. **83**, 4963 (2003).
[34] J. Wu, W. Walukiewicz, W. Shan, K. M. Yu, J. W. Ager III, S. X. Li, E. E. Haller, H. Lu, and W. J. Schaff, J. Appl. Phys. **94**, 4457 (2003).
[35] B. Arnaudov, T. Paskova, P. P. Paskov, B. Magnusson, E. Valcheva, B. Monemar, H. Lu, W. J. Schaff, H. Amano, and I. Akasaki, Phys. Rev. B **69**, 115216 (2004).
[36] R. Goldhahn, A. T. Winzer, V. Cimalla, O. Ambacher, C. Cobet, W. Richter, N. Esser, J. Furthmüller, F. Bechstedt, H. Lu, and W. J. Schaff, Superlattices Microstruct. **36**, 591 (2004).
[37] H. Jin, G. L. Zhao, and D. Bagayoko, J. Appl. Phys. **101**, 033123 (2007).
[38] *Numerical Data and Functional Relationships in Science and Technology*, Landolt-Börnstein New Series Vol. 17, edited by O. Madelung, M. Schulz, and H. Weiss (Springer, New York, 1982), Group III.
[39] C. P. Foley and T. L. Tansley, Phys. Rev. B **33**, 1430 (1986).
[40] P. Rinke, M. Winkelnkemper, A. Qteish, D. Bimberg, J. Neugebauer, and M. Scheffler, Phys. Rev. B **77**, 075202 (2008).
[41] P. Rinke, M. Scheffler, A. Qteish, M. Winkelnkemper, D. Bimberg, and J. Neugebauer, Appl. Phys. Lett. **89**, 161919 (2006).
[42] N. E. Christensen, I. Gorczyca, R. Laskowski, A. Svane, R. C. Albers, A. N. Chantis, T. Kotani, and M. van Schilfgaarde, Phys. Status Solidi B **246**, 570 (2009); A. Svane, N. E. Christensen, I. Gorczyca, M. van Schilfgaarde, A. N. Chantis, and T. Kotani (unpublished); the quasiparticle self-consistent GW method is described by S. V. Faleev, M. van Schilfgaarde, and T. Kotani, Phys. Rev. Lett. **93**, 126406 (2004); for a recent application to spin splitting in semiconductors, see A. N. Chantis, M. Cardona, N. E. Christensen, D. L. Smith, M. van Schilfgaarde, T. Kotani, A. Svane, and R. C. Albers, Phys. Rev. B **78**, 075208 (2008).
[43] D. Fritsch, H. Schmidt, and M. Grundmann, Phys. Rev. B **67**, 235205 (2003).
[44] I. Gorczyca, J. Plesiewicz, L. Dmowski, T. Suski, N. E. Christensen, A. Svane, C. S. Gallinat, G. Koblmueller, and J. S. Speck, J. Appl. Phys. **104**, 013704 (2008).

[45] Y. C. Yeo, T. C. Chong, and M. F. Li, J. Appl. Phys. **83**, 1429 (1998).
[46] S. Loughin, R. H. French, W. Y. Ching, Y. N. Xu, and G. A. Slack, Appl. Phys. Lett. **63**, 1182 (1993).
[47] A. Rubio, J. L. Corkill, M. L. Cohen, E. L. Shirley, and S. G. Louie, Phys. Rev. B **48**, 11810 (1993).
[48] C. Caetano, L. K. Teles, M. Marques, A. Dal Pino, Jr., and L. G. Ferreira, Phys. Rev. B **74**, 045215 (2006).
[49] L. K. Teles, L. M. R. Scolfaro, J. R. Leite, J. Furthmüller, and F. Bechstedt, J. Appl. Phys. **92**, 7109 (2002).
[50] M. Marques, L. K. Teles, L. M. R. Scolfaro, J. R. Leite, J. Furthmüller, and F. Bechstedt, Appl. Phys. Lett. **83**, 890 (2003).
[51] Y.-K. Kuo, B.-T. Liou, S.-H. Yen, and H.-Y. Chu, Opt. Commun. **237**, 363 (2004).
[52] L. K. Teles, J. Furthmüller, L. M. R. Scolfaro, J. R. Leite, and F. Bechstedt, Phys. Rev. B **63**, 085204 (2001).
[53] S. Yamaguchi, M. Kariya, S. Nita, T. Takeuchi, C. Wetzel, H. Amano, and I. Akasaki, Appl. Phys. Lett. **76**, 876 (2000).
[54] W. Terashima, S. B. Che, Y. Ishitani, and A. Yoshikawa, Jpn. J. Appl. Phys., Part 2 **45**, L539 (2006).
[55] P. Perlin, I. Gorczyca, T. Suski, P. Wisniewski, S. Lepkowski, N. E. Christensen, A. Svane, M. Hansen, S. P. DenBaars, B. Damilano, N. Grandjean, and J. Massies, Phys. Rev. B **64**, 115319 (2001).
[56] S. R. Lee, A. F. Wright, M. H. Crawford, G. A. Petersen, J. Han, and R. M. Biefeld, Appl. Phys. Lett. **74**, 3344 (1999).